NASA TECHNICAL NOTE

NASA TN D-4268

NASA TN D-4268

CALCULATED AND EXPERIMENTAL HINGE MOMENTS ON A TRAILING-EDGE FLAP OF A 75° SWEPT DELTA WING AT MACH 6

by J. Wayne Keyes and George C. Ashby, Jr.

Langley Research Center
Langley Station, Hampton, Va.

NATIONAL AERONAUTICS AND SPACE ADMINISTRATION • WASHINGTON, D. C. • DECEMBER 1967

CALCULATED AND EXPERIMENTAL HINGE MOMENTS ON A TRAILING-EDGE FLAP OF A 75° SWEPT DELTA WING AT MACH 6

By J. Wayne Keyes and George C. Ashby, Jr.

Langley Research Center
Langley Station, Hampton, Va.

NATIONAL AERONAUTICS AND SPACE ADMINISTRATION

For sale by the Clearinghouse for Federal Scientific and Technical Information
Springfield, Virginia 22151 – CFSTI price $3.00

CALCULATED AND EXPERIMENTAL HINGE MOMENTS ON A TRAILING-EDGE FLAP OF A 75° SWEPT DELTA WING AT MACH 6

By J. Wayne Keyes and George C. Ashby, Jr.
Langley Research Center

SUMMARY

The hinge-moment characteristics of a trailing-edge flap on a 75° swept delta wing have been investigated at a Mach number of 6.0 and a Reynolds number of 4.03×10^6 (based on the root chord of the delta wing). This investigation was conducted at angles of attack from 30° to 90° and flap-deflection angles from 0° to 30°. The boundary layer in the area of the wing-flap junction was considered to be transitional for angles of attack up to approximately 60° and laminar for angles of attack from 60° to 90°. Both a sharp and blunt leading-edge wing and two flap aspect ratios were used in the investigation.

Although the flow on the wing and flap was found to be complex, a meaningful analysis of the data can be made for the nonseparated case if the local flow regime over the wing and flap is properly classified (subsonic or supersonic) for each angle of attack and flap-deflection angle. The slope of the hinge-moment curves changed at approximately the same angle of attack that the flow regimes were predicted to change when tangent-cone and oblique-shock theories were used. The variation of the hinge-moment coefficient with angle of attack was predicted reasonably well by using oblique-shock theory for supersonic flow on the flap and an assumed parabolic pressure distribution for subsonic flow on the flap. These methods also gave a good indication of the actual pressure distribution on the flap. An abrupt increase in hinge-moment coefficient occurred when the bow-shock—flap-shock intersection was in the vicinity of the flap trailing edge. A strong shock was reflected from the shock intersection onto the flap; this shock caused a sharp rise in the pressure near the trailing edge and resulted in a rearward shift in the center of pressure. This abrupt change could cause dangerous control problems. Wing leading-edge bluntness and flap aspect ratio did not greatly affect the hinge-moment coefficient except when the bow-shock—flap-shock intersection was in the proximity of the flap trailing edge.

Boundary-layer separation over the flap was not extensive for flap deflections less than 20°. The type of boundary layer could have a strong influence on the hinge moments for flap-deflection angles large enough to cause boundary-layer separation.

INTRODUCTION

The delta wing has been cited in references 1 and 2 as having some advantages as a reentry vehicle over the complete reentry trajectory. Reentry into the atmosphere could be a high-angle-of-attack (80° to 90°) ballistic trajectory, a subsequent portion of the trajectory being flown with modulation from the maximum lift coefficient. Because the maximum lift coefficient occurs at an angle of attack near 50° for a delta wing (ref. 2), most of the trajectory could be flown in the moderate angle-of-attack range (30° to 60°).

The ability to modulate the lift coefficient for a delta-wing vehicle will probably require pivoting aerodynamic controls. To provide adequate torque for their deflection, knowledge of the aerodynamic hinge moments is required. No adequate method for predicting control hinge-moment characteristics for positively deflected trailing-edge flaps at hypersonic speeds has been developed. The investigation of reference 2 showed that the hinge moments of a trailing-edge flap on a 70° swept delta wing could be calculated reasonably well for negative flap-deflection angles; however, for positive deflection angles the investigation was limited to a positive angle of 10° and the agreement between the calculated and measured values was not as good.

The present program investigates the means for predicting the hinge-moment characteristics of a trailing-edge flap on a delta wing at positive deflection angles. For this purpose, hinge-moment coefficients were measured on two sizes of flaps on both a sharp and blunt leading-edge 75° swept delta wing. The investigation was conducted in the Langley 20-inch Mach 6 tunnel at angles of attack from 30° to 90° and flap deflections from 0° to 30°. Pertinent pressure distributions on the wing and flap were also obtained for angles of attack from 30° to 60° and flap-deflection angles from 0° to 30°.

SYMBOLS

A	flap aspect ratio
b	maximum span of delta wing, in. (cm)
b_f	flap span, in. (cm)
c	root chord of delta wing, in. (cm)
$C_{A,f}$	flap force coefficient component along wing chord axis
c_f	flap chord, in. (cm)
C_h	flap hinge-moment coefficient based on flap dimensions, $\frac{\text{Hinge moment}}{q_\infty S_f c_f}$

C_p	pressure coefficient
$(C_p)_{max}$	maximum pressure coefficient obtained from stagnation pressure behind a normal shock at Mach 6
M_∞	free-stream Mach number
$\frac{p_l}{p_\infty}$	ratio of local static pressure to free-stream static pressure
q_∞	free-stream dynamic pressure, psia (N/m^2)
r	radius of delta wing leading edge, in. (cm)
R_∞	Reynolds number based on free-stream conditions and root chord of delta wing
$\frac{S_f}{S_w}$	ratio of flap planform area to delta-wing planform area
x	chordwise coordinate, in. (cm)
y	spanwise coordinate, in. (cm)
α	angle of attack of delta-wing center line, deg
δ	flap-deflection angle, deg

APPARATUS, TESTS, AND MODELS

Tunnel

The Langley 20-inch Mach 6 tunnel is a blowdown type exhausting into the atmosphere. It can operate at stagnation pressures from about 7 to 37 atmospheres and stagnation temperatures up to 533° K. A more complete description of the tunnel is given in reference 3.

Sting and Support System

A model support sector rotates the model in the vertical plane of the test section at angles of attack from about -5° to 60°. For the force tests, the models were mounted

at an initial angle of 30°, relative to the sting, to avoid possible sting interference effects and to traverse angles of attack from 30° to 90° in a single sweep. For the pressure distributions a model injection system with a variable angle of attack was used.

Tests

The force tests were conducted at an absolute stagnation pressure of about 21.4 atmospheres and a free-stream Reynolds number of 4.03×10^6 (based on the root chord of the delta wing). Tunnel stagnation temperature was maintained at about 478° K to avoid liquefaction of the air. The model angle of attack varied from 30° to 90° at trailing-edge flap deflections of 0°, 10°, 20°, and 30°. The pressure tests were conducted at the same stagnation pressure, but at a higher stagnation temperature (533° K). For these conditions the Reynolds number was 3.36×10^6 (based on the root chord of the delta wing). The pressure model angle of attack varied from 30° to 60° with flap-deflection angles from 0° to 30°.

Models

A sketch of the assembled model showing the location of the hinge-moment balance and the gap seal is presented in figure 1(a). The design dimensions of the two delta wings and flaps are shown in figure 1(b). Pressure orifice locations on the wing and flap are given in figure 1(c). Both wings have a leading-edge sweep of 75°. The leading edge of one wing had a sharp 15° double-wedge cross section ($r/c \approx 0$) and the other, a semicircular cross section ($r/c = 0.016$). The delta wing with the cylindrical leading edge had a sharp prow. The planform area S_w of the delta wings was 17.149 in^2 (110.638 cm^2). The trailing-edge flap was attached to the balance at the wing midspan with the balance axis normal to the wing at the hinge line. The gap between the trailing edge of the delta wing and the flap was maintained at 0.006 inch (0.015 cm) and the gap was sealed by using a 0.060-inch-diameter (0.152-cm) rubber gasket inserted in a groove on the trailing edge of the wing. (See fig. 1(b).)

The flaps were two sizes: $S_f/S_w = 0.2$ and $S_f/S_w = 0.3$. The flap span was constant and equal to the maximum span of the flat portion of the sharp-leading-edge delta wing. The chord was varied to change aspect ratio. The pressure flap $\left(S_f/S_w = 0.3\right)$ was similar to the force flap except that it was attached to the delta wing by two brackets instead of a balance. The flap was drilled for 0.040-inch (0.102-cm) inside diameter tubing which was increased to 0.070-inch (0.178-cm) inside diameter to reduce lag effects. A photograph of the force model on a sting is shown in figure 2.

Tests with the same gap setting but no gasket showed no appreciable differences in the measured hinge moments. Therefore, only the data obtained with the sealed gap are presented.

MEASUREMENTS AND ACCURACY

The hinge moment and the flap force component along the wing chord axis were measured by a two-component strain-gage balance. The force and moment coefficients are referred to the axis system shown in figure 1(a) and are based on the flap chord and area. The hinge line was located at the junction of the bottom surfaces of the wing and flap. The balance pitch center was located directly above the hinge line; this location allowed the moment transfer to be accomplished by using only the flap force component along the wing chord axis. An optical system described in reference 4 was used to set the angle of attack. Individual pressure transducers with an accuracy of 0.5 percent of full scale were used to measure the local pressure on the wing and flap.

Based on instrument calibrations and repeatability of data the estimated accuracies are:

	$S_f/S_w = 0.2$	$S_f/S_w = 0.3$
C_h	±0.048	±0.020
α, deg	±0.10	
δ, deg	±0.05	
M_∞	±0.02	

PRESENTATION OF RESULTS

The variation of hinge-moment coefficient with angle of attack at a given flap-deflection angle is presented in figure 3 along with calculated values obtained from several theoretical and empirical methods. Figure 4 includes typical schlieren photographs. Figures 5 and 6 show typical pressure distributions on the wing and flap. The measured hinge-moment coefficients are compared, in figure 7, with those obtained by integrating the measured pressures. Figures 8 and 9 show the effects of wing leading-edge bluntness and flap aspect ratio, respectively, on the hinge-moment coefficient. A cross plot of the variation of hinge-moment coefficient with flap-deflection angle for a given angle of attack is presented in figure 10.

DISCUSSION

Flow Characteristics

In general, the hinge-moment coefficient of a trailing-edge flap on a delta wing is determined by the local flow conditions, which are affected by the angle of attack, flap-deflection angle, bow-shock—flap-shock interaction, and type of boundary-layer separation (laminar, transitional, or turbulent). The influences of these phenomena on the hinge-moment characteristics are discussed in subsequent sections.

Local flow conditions.- To analyze the hinge-moment characteristics of the flap, the flow over the delta wing and flap was first classified according to the local flow regimes. These flow regimes which are similar to those of references 5 and 6 are: (1) supersonic on the wing and flap, (2) supersonic on the wing and subsonic on the flap, and (3) subsonic on both the wing and flap. The flow over the windward surface of a delta wing is conical in nature for the angle-of-attack range from 30° to 60°; therefore, the tangent-cone theory was used to determine the flow properties along the wing center line. These flow properties in conjunction with oblique-shock theory were used to compute the flap characteristics.

The calculated angles of attack for the various flow regimes are shown for each flap deflection in figure 3. Typical measured pressure distributions for the various flow regimes are shown in figure 5. Figures 5(a) and 5(e) are examples of complete supersonic and subsonic flow, respectively, on the wing and flap. The flow fields illustrated in figures 5(b) to 5(d) are complicated by the bow-shock—flap-shock intersection.

At low angles of attack and at the conditions of these tests the bow-shock—flap-shock intersection occurs downstream of the trailing edge of the flap. As the angle of attack increases, however, this intersection moves closer to the flap and eventually moves in front of the flap. An expansion or a compression wave is reflected from this intersection as shown in the following sketch:

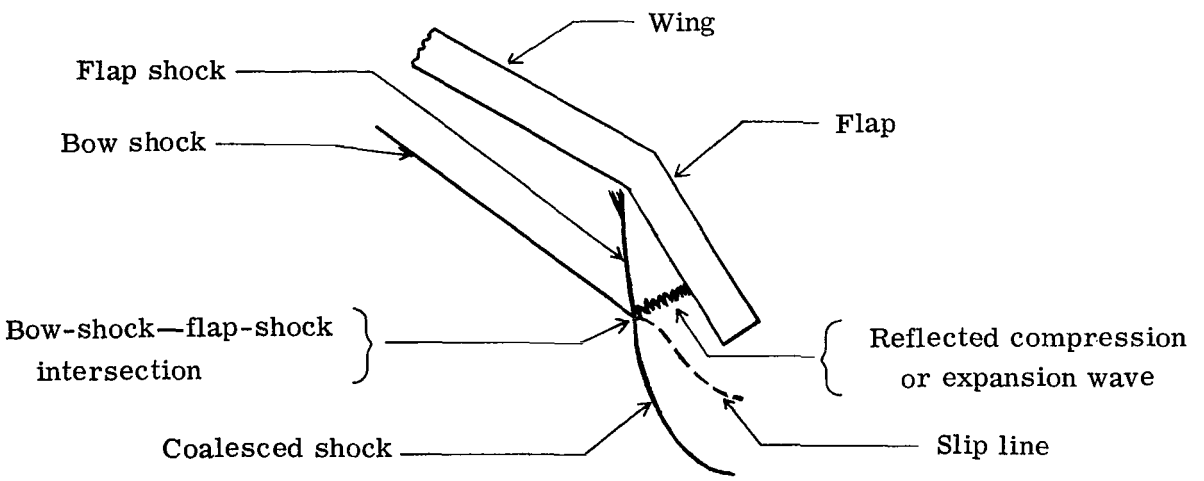

When this intersection occurs as shown in the sketch, the reflected wave can influence the pressure distribution on the flap and therefore the hinge moment. The schlieren photographs of figures 4(b), 5(b), and 5(c) show that, in general (for the present tests), a strong shock is reflected from the bow-shock—flap-shock intersection. As the angle of attack is increased, the reflected compression wave should probably first increase the

pressure level at the trailing edge (as in fig. 5(b)) and thus shift the center of pressure of the flap rearward. This center-of-pressure shift would cause an increase in the hinge moment. As α increased further, the reflected wave influence would probably move forward on the flap; however, as shown in the schlieren photograph of figure 5(c), the flow field becomes very complex and it is difficult to determine the minute details of the flow. The abrupt change in the hinge moment as observed in figure 3 (that is, from $\alpha = 45^{\circ}$ to $\alpha = 47.5^{\circ}$ for $\delta = 10^{\circ}$) is evidently caused by the reflected wave at the bow-shock—flap-shock intersection. This abrupt change is severe (approximately 40-percent increase for $\delta = 20^{\circ}$) and could cause dangerous control operation problems. Because of the large increment in angle of attack, this rapid change in the hinge moment was not detected in reference 2 at $\delta = 10^{\circ}$.

The angles of attack for which the bow-shock—flap-shock intersection moves upstream of the flap trailing edge were obtained from the schlieren photographs and are identified by the positive-sloping hatched marks in figure 3. The calculated angles of attack for which the shock intersection occurs in front of the trailing edge of the flap were obtained by using the theoretical shock angles and the geometry of the model and are identified by the negative-sloping hatched mark in figure 3. The observed and predicted values agree for $\delta = 10^{\circ}$; however, for $\delta = 20^{\circ}$, this intersection occurred at a lower angle of attack than that calculated. This difference is possibly a result of boundary-layer separation and/or flow equilibrium requirements at the shock intersection. There is also a possibility of flow unsteadiness when the shock intersection moves in front of the flap and in the area of the wing-flap junction as noted in reference 7.

Boundary-layer separation.- Unpublished heat-transfer data obtained on a model similar to the pressure model (tested under the present conditions) along with calculated heat-transfer data indicate that the boundary layer is transitional in the area of the wing-flap junction from $\alpha \approx 30^{\circ}$ to $\alpha \approx 60^{\circ}$. Heat-transfer data obtained for angles of attack beyond 60° (subsonic flow on wing and flap) indicate that the boundary layer may be laminar up to 90°. Similar results were observed in references 8 and 9.

Boundary-layer separation occurs on the wing and flap for a flap-deflection angle of 30° up to approximately an angle of attack of 50° as shown in the schlieren photograph of figure 4(c) and the pressure distribution of figure 6. Since the boundary layer in the area of the flap is transitional and nearly turbulent, the data of figure 9(a) of reference 10 indicate that the maximum deflection angle for attached flow is approximately 23° for a flat plate and wedge at a local Mach number of 2.70 (tangent-cone value at $\alpha = 30^{\circ}$). Therefore, separation should occur at some deflection angle below 30° for the delta-wing flap configuration at $\alpha = 30^{\circ}$. A comparison of the data in figures 6 and 5(b) at $\alpha = 30^{\circ}$ shows that separation has occurred for $\delta = 30^{\circ}$, but has not occurred for $\delta = 20^{\circ}$. However, it can be seen in figure 5(c) that a slight separated region exists at $\alpha = 40^{\circ}$ and $\delta = 20^{\circ}$.

The separation along with the influence of the bow-shock—flap-shock interaction tends to cause the hinge-moment coefficient to remain nearly constant at the lower angles of attack ($\alpha = 30^{\circ}$ to $\alpha = 37.5^{\circ}$) for $\delta = 30^{\circ}$ (fig. 3). Separation also tends to delay the onset of subsonic flow on the flap since the angle of the separation "ramp" is less than that of the flap-deflection angle.

Figure 6 shows a comparison of the measured and calculated values of pressure on the wing, in the separated region, and on the flap. For the wing and separated region, the calculated values give a good indication of the level of the measured pressures. However, the calculated pressure on the flap was only in fair agreement with the maximum measured pressure on the flap. Tangent-cone theory was used to calculate the pressure level on the wing; the first peak pressure in the separated region was calculated by using equation (6) of reference 11 (which is for turbulent flow); and the pressure level on the flap was calculated by assuming that the flow passes through both the separation shock and the flap shock. The good agreement of the measured and calculated first peak pressure in the separated region indicates that the boundary layer at the wing-flap junction is close to being fully turbulent.

At this point it should be noted that the results of this investigation, especially at the higher deflection angles, could be strongly affected by a change in the type of boundary layer. Either a fully laminar or turbulent boundary layer could alter the separation characteristics at a given deflection angle and thereby affect the flap pressure distribution in at least two ways. The first would be the direct effect on the peak pressure and its location; the second would be the indirect effect by its influence on the location of and conditions at the bow-shock—flap-shock intersection. Because the influence of this intersection on the flap hinge moment can be severe but is strongly dependent on a particular combination of conditions, the effect of the change in the boundary layer may have a significant effect on the hinge-moment characteristics.

Comparison of measured and calculated data.- A comparison of the measured and calculated hinge-moment coefficients obtained from several methods is presented in figure 3. In all cases a constant spanwise pressure distribution was assumed. The hinge-moment coefficients predicted from modified Newtonian theory $\left((C_p)_{max} = 1.818\right)$ show the usual results; that is, the best agreement is obtained when the flow passes through only one shock. This result occurs for all angles of attack where $\delta = 0^{\circ}$ and for the other deflection angles at angles of attack where the flow is subsonic on the wing and flap.

The other methods used to calculate the chordwise pressure distribution on the flap were dictated by the combinations of flow regimes on the wing and flap as determined from the tangent-cone and oblique-shock theories, respectively. For the combination of supersonic flow on both the wing and flap and the bow-shock—flap-shock intersection downstream of the flap, the pressures used for the flap were the constant values predicted by

oblique-shock theory. The hinge moments obtained from the integration of these predicted pressures give a good estimate of both the values and trends with angle of attack (see fig. 3) for the 0° and 10° deflection angles. At $\delta = 20^{\circ}$, the shock intersection occurs in front of the flap at an angle of attack less than that predicted. Since this condition causes an abrupt increase in the hinge moment, the values predicted with the use of the oblique-shock theory are too low.

When the shock intersection moves in front of the flap, a solution of the triple point is required to determine whether a compression or expansion wave is reflected from the shock intersection. This solution was not made for the present investigation because of the complexity of the flow. However, as mentioned previously, the schlieren photographs show that a strong shock is reflected from the shock intersection.

By using the schlieren photographs to locate the position of the reflected shock at each angle of attack, the hinge moments were calculated in the following manner: The pressure distribution and Mach number for the portion of the flap forward of the reflected shock was that obtained from tangent-cone—oblique-shock theory. The pressure rise across the shock was assumed to be that across a normal shock at the theoretical flap Mach number. Since the flow behind a normal shock is subsonic, the pressure distribution over the aft portion of the flap was assumed to decrease parabolically to either the static pressure behind the coalesced bow and flap shocks (which is shown by the schlieren photographs to be nearly normal) or that for sonic velocity at the trailing edge, whichever was the lesser. As indicated by the x symbols in figure 3, the trend of the hinge moment under the influence of the shock intersection is well predicted by this method.

For $\delta = 0^{\circ}$ and the condition of subsonic flow on the wing and flap, the local pressure was assumed to be constant and equal to the static pressure behind a normal shock at Mach 6. For the flap deflected and subsonic flow on the flap, the local pressure was assumed to decrease parabolically from the flap hinge line to the trailing edge. This method, which was found to be fairly satisfactory in references 5 and 6, assumes that the flow in the subsonic region ahead of the flap (behind the flap normal shock for supersonic flow on the wing and behind the bow shock for subsonic flow on the wing) decelerates isentropically along the wing chord to a stagnation value at the hinge line. The local pressure then is assumed to decrease on the flap parabolically from this stagnation value to either the static pressure behind the coalesced bow and flap shocks or the pressure for sonic velocity at the trailing edge, whichever was the lesser. The hinge moments obtained from the integration of these pressure distributions follow the trends of the measured values very well and the agreement between the two is, in general, reasonably good.

Since the hinge moment involves both an integrated force and the center of pressure, good agreement between the measured and calculated value could possibly be fortuitous. However, a comparison of the theoretical and measured pressure distributions of figure 5

for deflection angles of 10° and 20° shows that the theories and assumptions predicted the measured pressures reasonably well. The pressures on the wing are constant spanwise at least over the center portion and the values are well predicted by tangent-cone theory. The pressures on the flap are shown to drop only slightly in the spanwise direction except near the edge. The oblique-shock theory for supersonic flow on the flap (fig. 5(a)) predicts the pressure level very well. When the flow is subsonic on the flap, the assumed parabolic pressure distribution is a reasonably good representation; however, the calculated and experimental pressure level are only in fair agreement.

Comparison of measured and integrated C_h.- The values of hinge-moment coefficient obtained from the integrated measured pressure distribution agreed very well with the measured hinge-moment coefficient (fig. 7). The pressure on the leeward side of the flap used for these calculations was derived from the expression $C_p = -\frac{1}{M_\infty{}^2}$ as presented in reference 12.

Variation of Parameters

Leading-edge bluntness.- In general, there is little effect of leading-edge bluntness on the hinge-moment coefficient except when the bow-shock—flap-shock intersection is in the proximity of the flap trailing edge (fig. 8).

Flap aspect ratio.- There is only a slight effect of flap aspect ratio on the hinge-moment coefficient except when the bow-shock—flap-shock intersection is in the proximity of the flap trailing edge. (Note, for example, $\alpha = 45^{\circ}$ and $\delta = 10^{\circ}$, fig. 9(a).) The intersection is in this position at a lower angle of attack for the lower aspect ratio flap (A = 2.143). Therefore, the marked increase in hinge-moment coefficient due to the reflected shock from the intersection usually occurs at a lower angle of attack (fig. 9(a), $\delta = 10^{\circ}$ and $\alpha = 45^{\circ}$ for the low aspect ratio and $\alpha = 47.5^{\circ}$ for the high aspect ratio). Since the effect of the shock intersection on the hinge-moment coefficient is similar for both aspect ratio flaps, it would be expected that the curves for the two would be displaced under these effects up to the angle of attack for subsonic flow on the wing.

Flap-deflection angle.- The hinge-moment data of figure 3 are cross plotted in figure 10 to show the effect of flap-deflection angles at a given angle of attack. The shock-intersection and boundary-layer-separation effect apparently distorts the nearly linear variation with deflection angle when α increases from 30° to 35°. It should be noted that the abrupt changes in hinge-moment coefficient for the deflection-angle change in the region of $10^{\circ} < \delta < 20^{\circ}$ at $\alpha = 35^{\circ}$ might not be the maximum that could occur. A larger change may have been observed if smaller increments of angles of attack and deflection angles were used. The change in the trend of the $\alpha = 50^{\circ}$ curve at $\delta = 10^{\circ}$ shows the effect of subsonic flow on the flap.

CONCLUSIONS

Hinge-moment data of a positively deflected trailing-edge flap on a 75° swept delta wing have been analyzed. The test Mach number was 6.0 with a Reynolds number of 4.03×10^6 and an angle-of-attack range from 30° to 90°. The boundary layer in the vicinity of the wing-flap junction was considered to be transitional up to approximately 60° angle of attack and laminar from 60° to 90°. Results of this investigation indicate the following conclusions:

Without Boundary-Layer Separation

1. Although the flow over the wing and flap was found to be complex, a meaningful analysis of the data can be made if the local flow over the wing and flap is classified into the proper flow regime for each angle of attack and flap-deflection angle. These flow regimes are (1) supersonic on the wing and flap, (2) supersonic on the wing and subsonic on the flap, and (3) subsonic on both the wing and flap.

2. The slope of the hinge-moment curves changed at approximately the same angle of attack that the flow regimes were predicted to change with the use of tangent-cone and oblique-shock theories.

3. An abrupt, and perhaps dangerous, increase in hinge-moment coefficient was found to occur when the bow-shock—flap-shock intersection was in the vicinity of the flap trailing edge.

4. The variation of the hinge-moment coefficient with angle of attack was predicted reasonably well with the use of oblique shock theory for supersonic flow on the flap and an assumed parabolic pressure distribution for subsonic flow on the flap. These methods also gave a good indication of the actual pressure distribution on the flap.

5. Wing leading-edge bluntness and flap aspect ratio only affected the hinge-moment coefficient when the bow-shock—flap-shock intersection was in the proximity of the flap trailing edge.

With Boundary-Layer Separation

1. Boundary-layer separation over the flap was not extensive at or below a deflection angle of 20° at any angle of attack. The boundary-layer separation (at a deflection angle of 30°) in conjunction with the shock intersection effects had a tendency to reduce the hinge moments.

2. Although the experimental data were obtained at only one Reynolds number, the known differences in the extent of separation and in the peak pressure rise for laminar, transitional, and turbulent boundary layers allow the conclusion to be made that the type

of boundary layer could have a strong influence on the hinge-moment characteristics at deflection angles large enough to permit boundary-layer separation.

Langley Research Center,
National Aeronautics and Space Administration,
Langley Station, Hampton, Va., January 20, 1967,
126-13-03-18-23.

REFERENCES

1. Staff of Langley Flight Research Division (Compiled by Donald C. Cheatham): A Concept of a Manned Satellite Reentry Which Is Completed With a Glide Landing. NASA TM X-226, 1959.

2. Fetterman, David E.; and Neal, Luther, Jr.: An Analysis of the Delta-Wing Hypersonic Stability and Control Behavior at Angles of Attack Between 30° and 90°. NASA TN D-1602, 1963.

3. Sterrett, James R.; and Emery, James C.: Extension of Boundary-Layer-Separation Criteria to a Mach Number of 6.5 By Utilizing Flat Plates With Forward-Facing Steps. NASA TN D-618, 1960.

4. Ashby, George C., Jr.; and Fitzgerald, Paul E., Jr.: Longitudinal Stability and Control Characteristics of Missile Configurations Having Several Highly Swept Cruciform Fins and a Number of Trailing-Edge and Fin-Tip Controls at Mach Numbers From 2.21 to 6.01. NASA TM X-335, 1961.

5. Staylor, W. Frank; Sterrett, James R.; and Goldberg, Theodore J.: Pressure Distributions on a Blunt-Nose Lifting Reentry Body With Flaps at a Mach Number of 6.0 With Emphasis on the Nature of the Local Flow. NASA TM X-766, 1963.

6. Holloway, Paul F.: Comparison of Experimental Control Effectiveness of a Flat-Bottom Canted-Nose Half-Cone Reentry Configuration With That Obtained by Several Methods of Prediction for Various Types of Local Flow at a Mach Number of 6.0. NASA TM X-767, 1963.

7. Stern, I.; and Rowe, W. H., Jr.: The Effect of Gap Size on Pressure and Heating Over the Flap of a Blunt Delta Wing in Hypersonic Flow. AIAA Paper No. 66-408, Am. Inst. Aeron. Astronaut., June 1966.

8. Dunavant, James C.: Investigation of Heat Transfer and Pressures on Highly Swept Flat and Dihedraled Delta Wings at Mach Numbers of 6.8 and 9.6 and Angles of Attack to 90°. NASA TM X-688, 1962.

9. Paulsen, James J.; and Schadt, Gail H.: A Study of the Pressure and Heat Transfer Distribution on Highly Swept Slab Delta Wings in Supersonic Flow. AIAA Paper No. 66-130, Am. Inst. Aeron. Astronaut., Jan. 1966.

10. Sterrett, James R.; and Emery, James C.: Experimental Separation Studies for Two-Dimensional Wedges and Curved Surfaces at Mach Numbers of 4.8 to 6.2. NASA TN D-1014, 1962.

11. Love, Eugene S.: Pressure Rise Associated With Shock-Induced Boundary-Layer Separation. NACA TN 3601, 1955.

12. Mayer, John P.: A Limit Pressure Coefficient and an Estimation of Limit Forces on Airfoils at Supersonic Speeds. NACA RM L8F23, 1948.

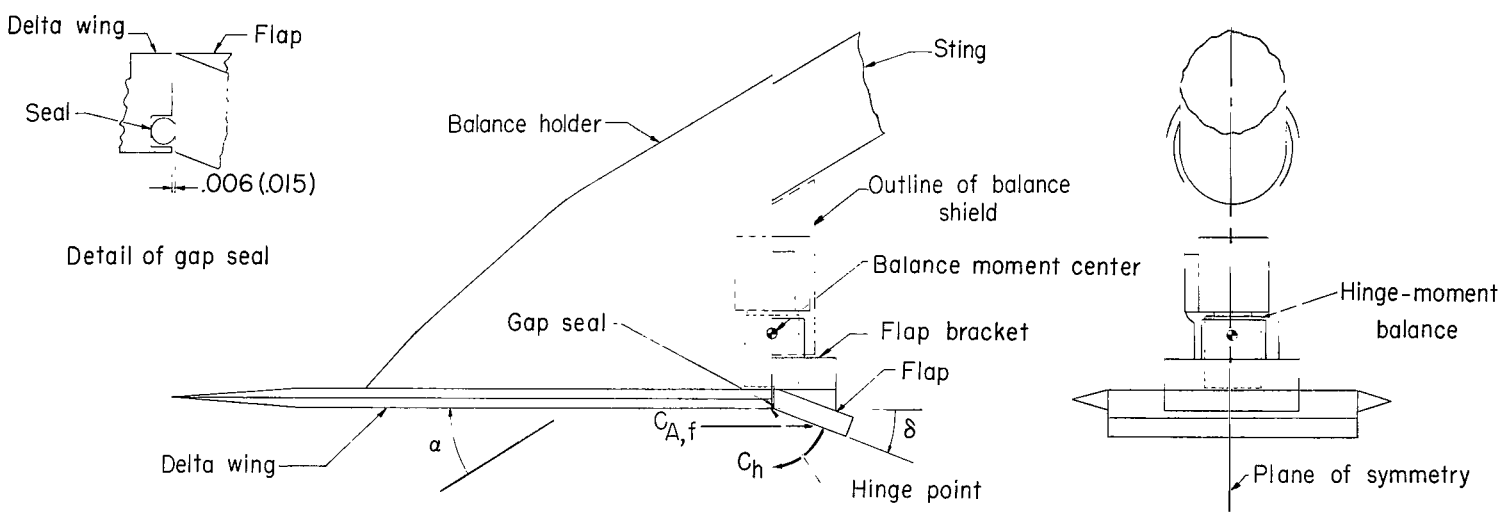

(a) Model assembly showing location of hinge-moment balance.

Figure 1.- Model configuration. All dimensions are in inches (centimeters).

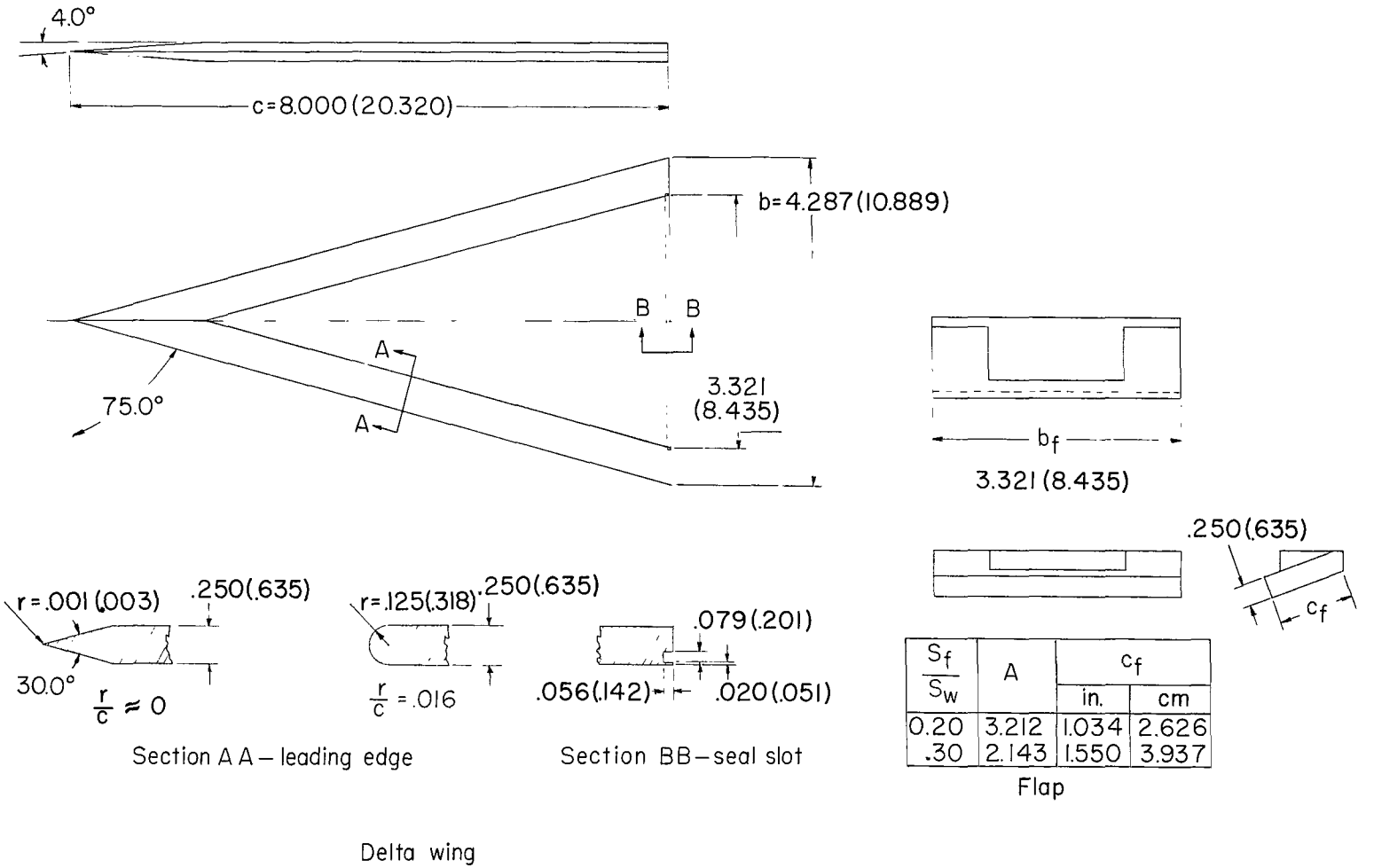

S_f/S_w	A	c_f	
		in.	cm
0.20	3.212	1.034	2.626
.30	2.143	1.550	3.937

Flap

(b) Delta wing and flap.

Figure 1.- Continued.

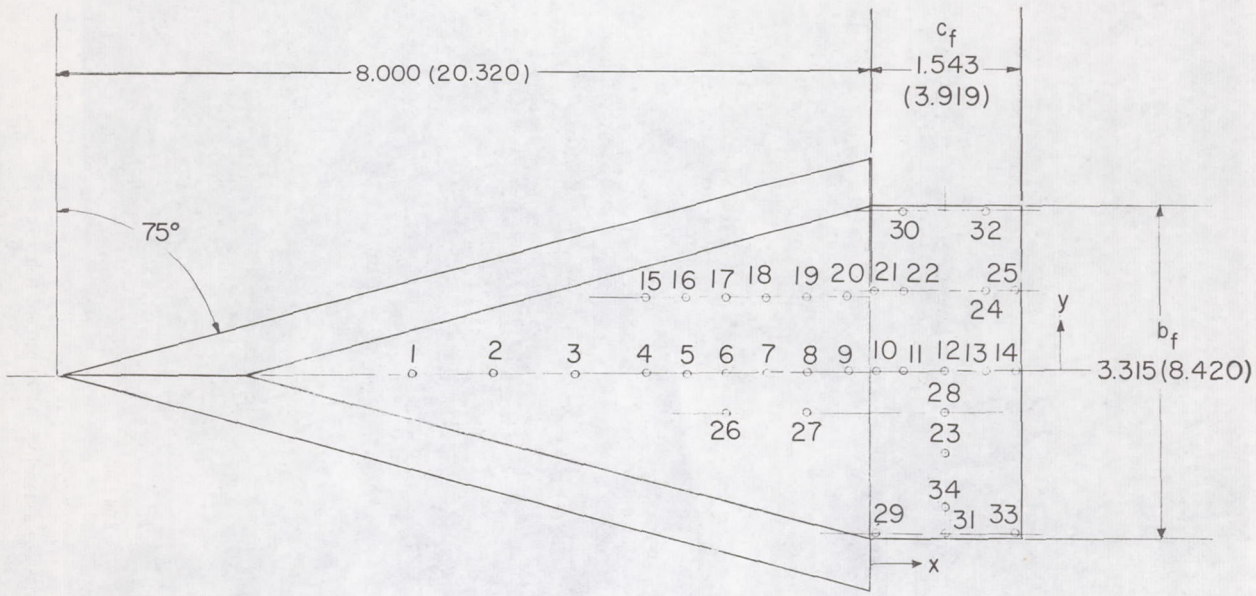

Orifice	$\frac{x}{c_f}$	$\frac{y}{b_f}$	Orifice	$\frac{x}{c_f}$	$\frac{y}{b_f}$	Orifice	$\frac{x}{c_f}$	$\frac{y}{b_f}$
1	-2.918	0	14	0.968	0	27	-0.388	-0.120
2	-2.393	↓	15	-1.428	.228	28	.510	-.113
3	-1.881	↓	16	-1.167	↓	29	.036	-.481
4	-1.428	↓	17	-.907	↓	30	.250	↓
5	-1.169	↓	18	-.647	↓	31	.503	↓
6	-.907	↓	19	-.388	↓	32	.754	↓
7	-.647	↓	20	-.125	↓	33	.970	↓
8	-.598	↓	21	-.034	.247	34	.502	-.402
9	-.129	↓	22	.240	↓			
10	.036	↓	23	.504	-.234			
11	.247	↓	24	.760	.255			
12	.499	↓	25	.967	↓			
13	.752	↓	26	-.907	-.120			

(c) Pressure model orifice locations.

Figure 1.- Concluded.

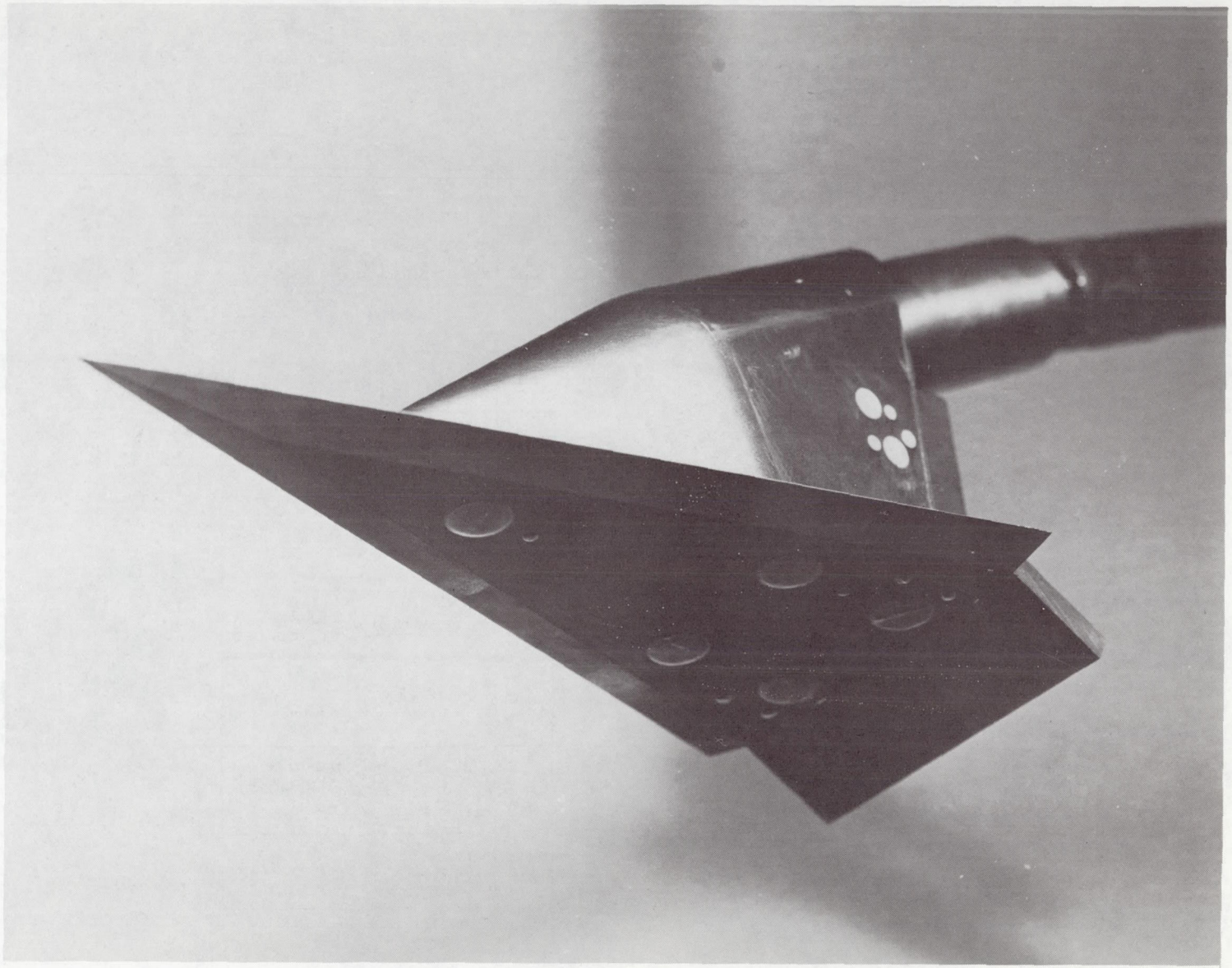

Figure 2.- Photograph of sharp-leading-edge delta wing and 20-percent flap.

L-66-5074

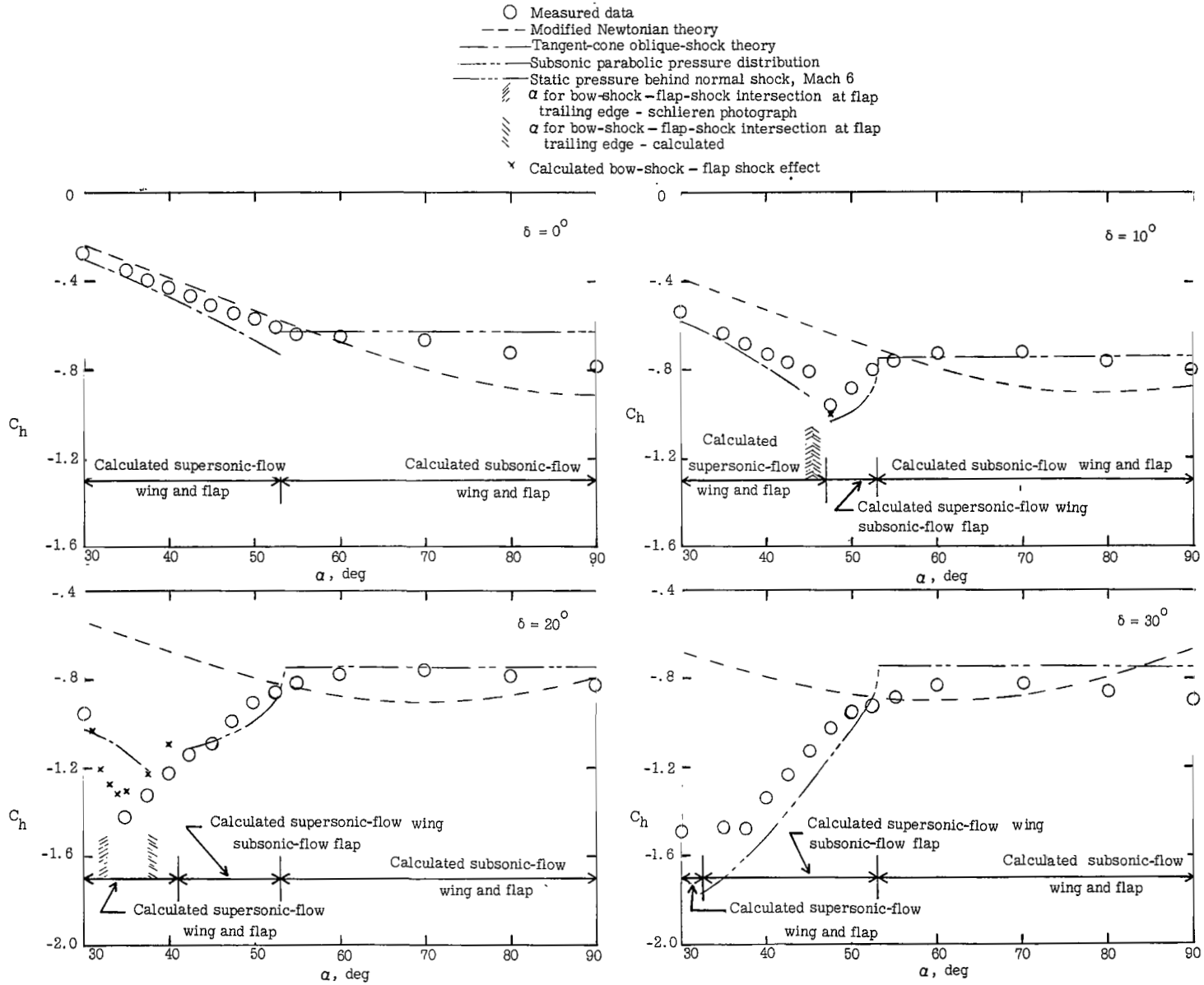

Figure 3.- Variation of hinge-moment coefficient with angle of attack for a given control deflection. $r/c \approx 0$; $A = 3.212$.

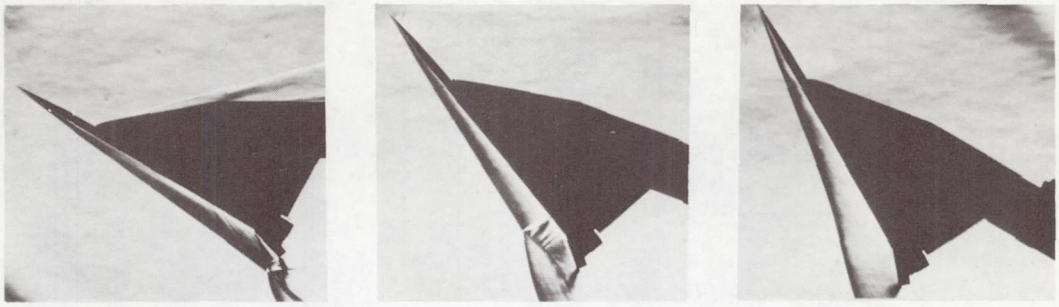

$\alpha = 30°$ (Supersonic-flow wing and flap)

$\alpha = 50°$ (Supersonic-flow wing, subsonic-flow flap)

$\alpha = 60°$ (Subsonic-flow wing and flap)

(a) Calculated flow regimes; $\delta = 20^{0}$.

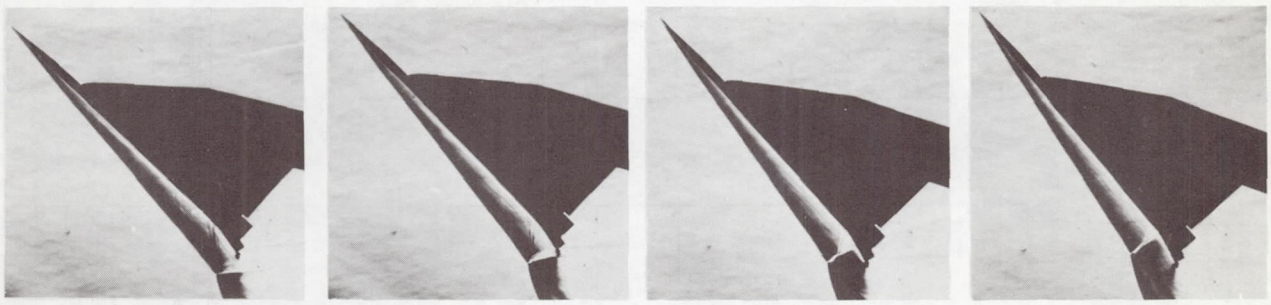

$\alpha = 42.5°$ $\alpha = 45°$ $\alpha = 47.5°$ $\alpha = 50°$

(b) Bow-shock—flap-shock intersection; $\delta = 10^{0}$.

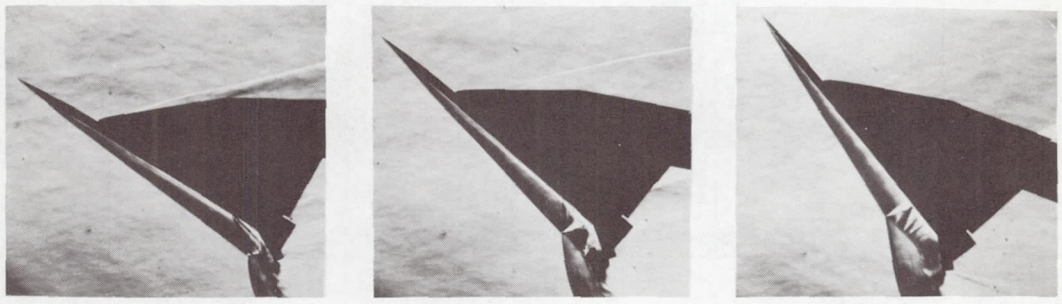

$\alpha = 30°$ $\alpha = 40°$ $\alpha = 50°$

(c) Separated flow; $\delta = 30^{0}$. L-67-953

Figure 4.- Typical schlieren photographs of force model; $r/c \approx 0$; $A = 3.212$.

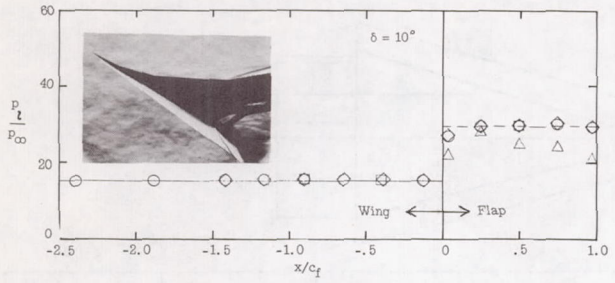

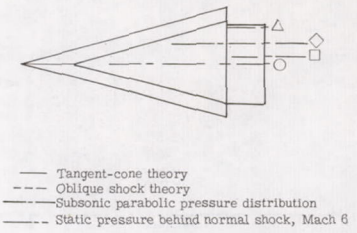

(a) $\alpha = 30^0$. Calculated and measured supersonic flow on wing and flap.

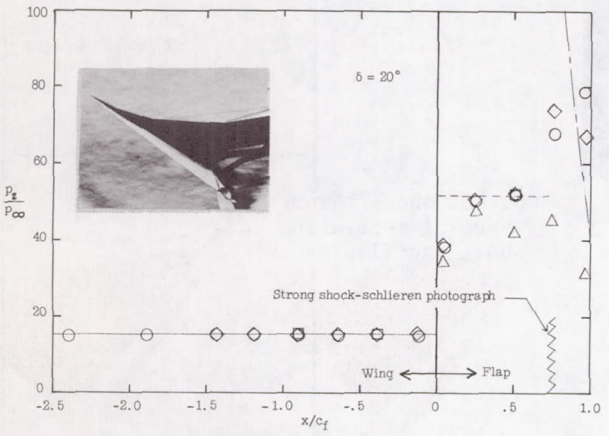

(b) $\alpha = 30^0$. Calculated supersonic flow on wing and flap. (Flow on flap complicated by bow-shock—flap-shock intersection.)

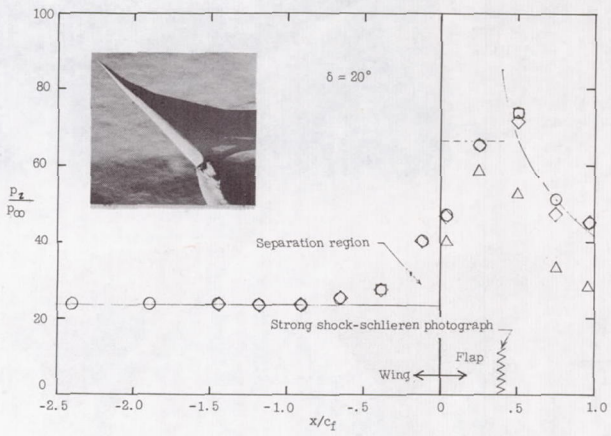

(c) $\alpha = 40^0$. Calculated supersonic flow on wing and flap. (Flow on flap complicated by bow-shock—flap-shock intersection and separation.)

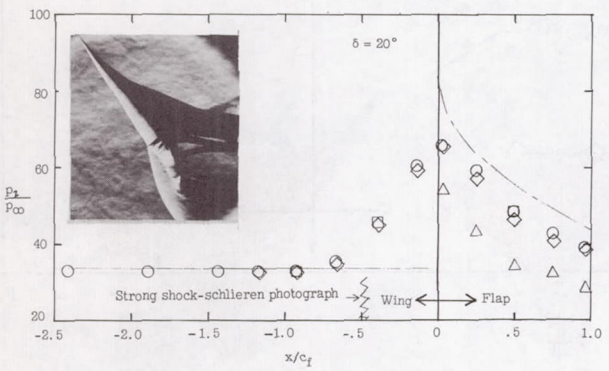

(d) $\alpha = 50^0$. Calculated supersonic flow on wing, subsonic flow on flap.

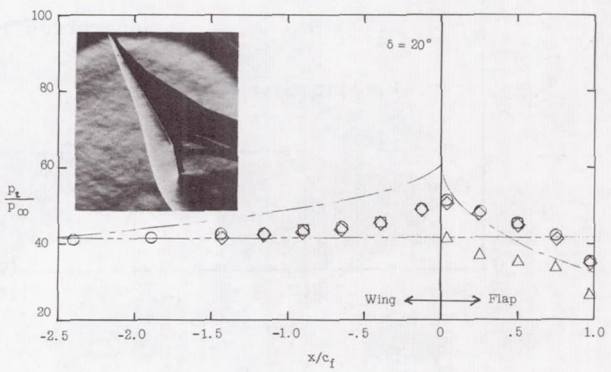

L-67-954

(e) $\alpha = 60^0$. Calculated and measured subsonic flow on wing and flap.

Figure 5.- Typical pressure distributions on delta wing and flap. A = 2.143; $r/c \approx 0$; and $R_\infty = 3.36 \times 10^6$.

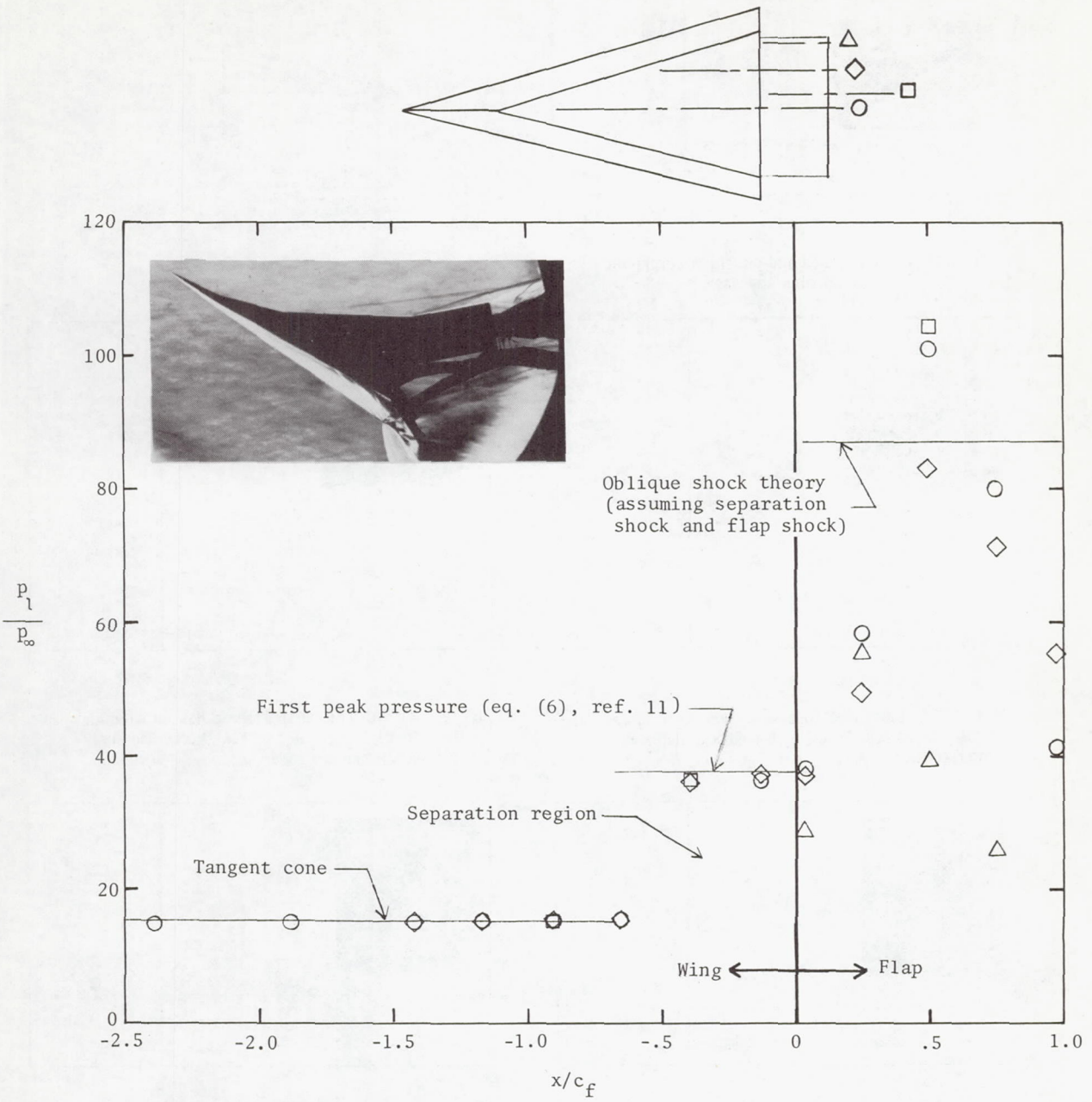

L-67-955

Figure 6.- Pressure distribution on delta wing and flap showing region of separation. $\alpha = 30^0$; $\delta = 30^0$; $A = 2.143$; $r/c \approx 0$; and $R_\infty = 3.36 \times 10^6$.

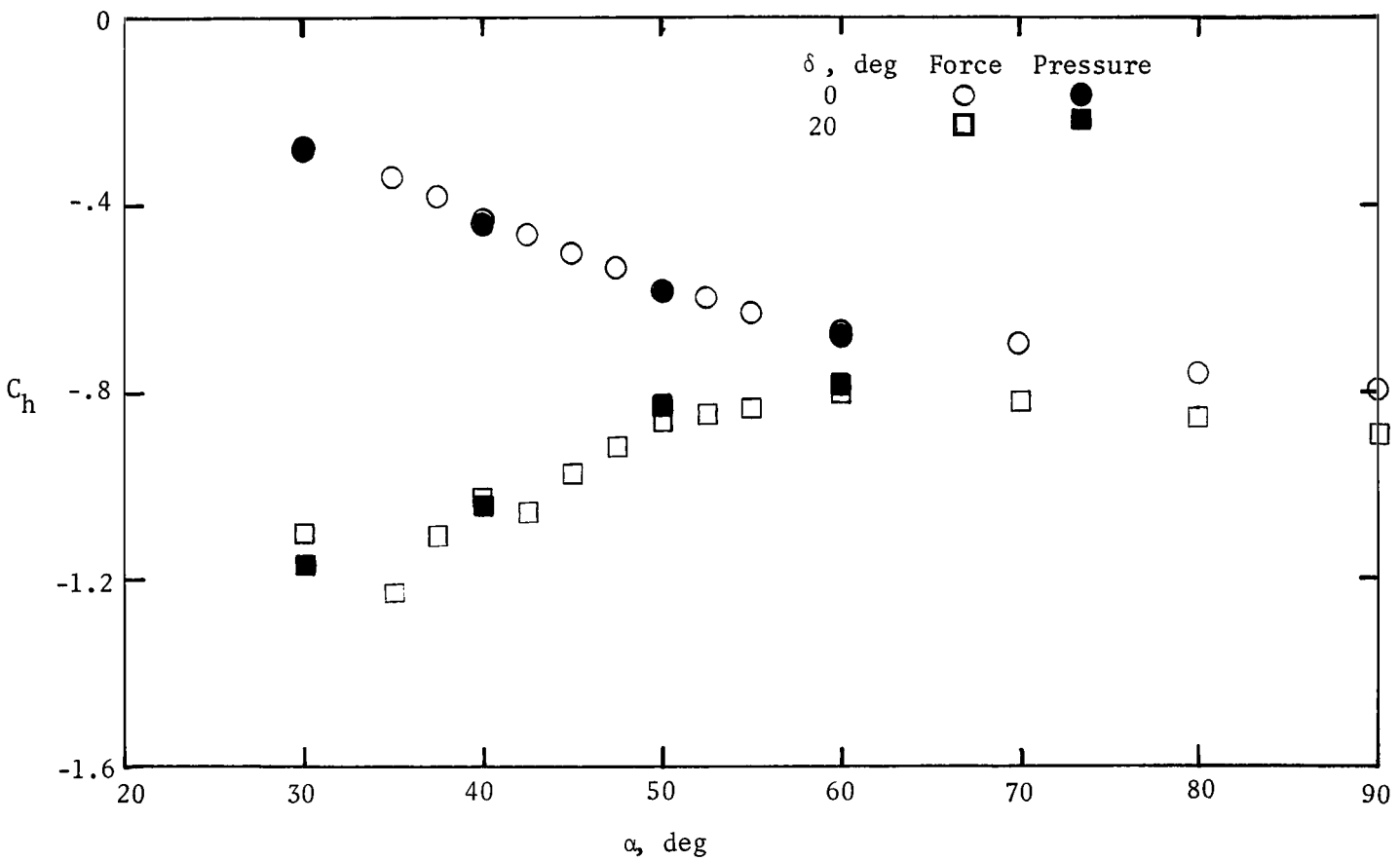

Figure 7.- Comparison of measured hinge-moment coefficient with integrated measured pressure distribution. For force measurements, $R_\infty = 4.03 \times 10^6$; for the integrated pressures, $R_\infty = 3.36 \times 10^6$. $r/c \approx 0$; $A = 2.143$.

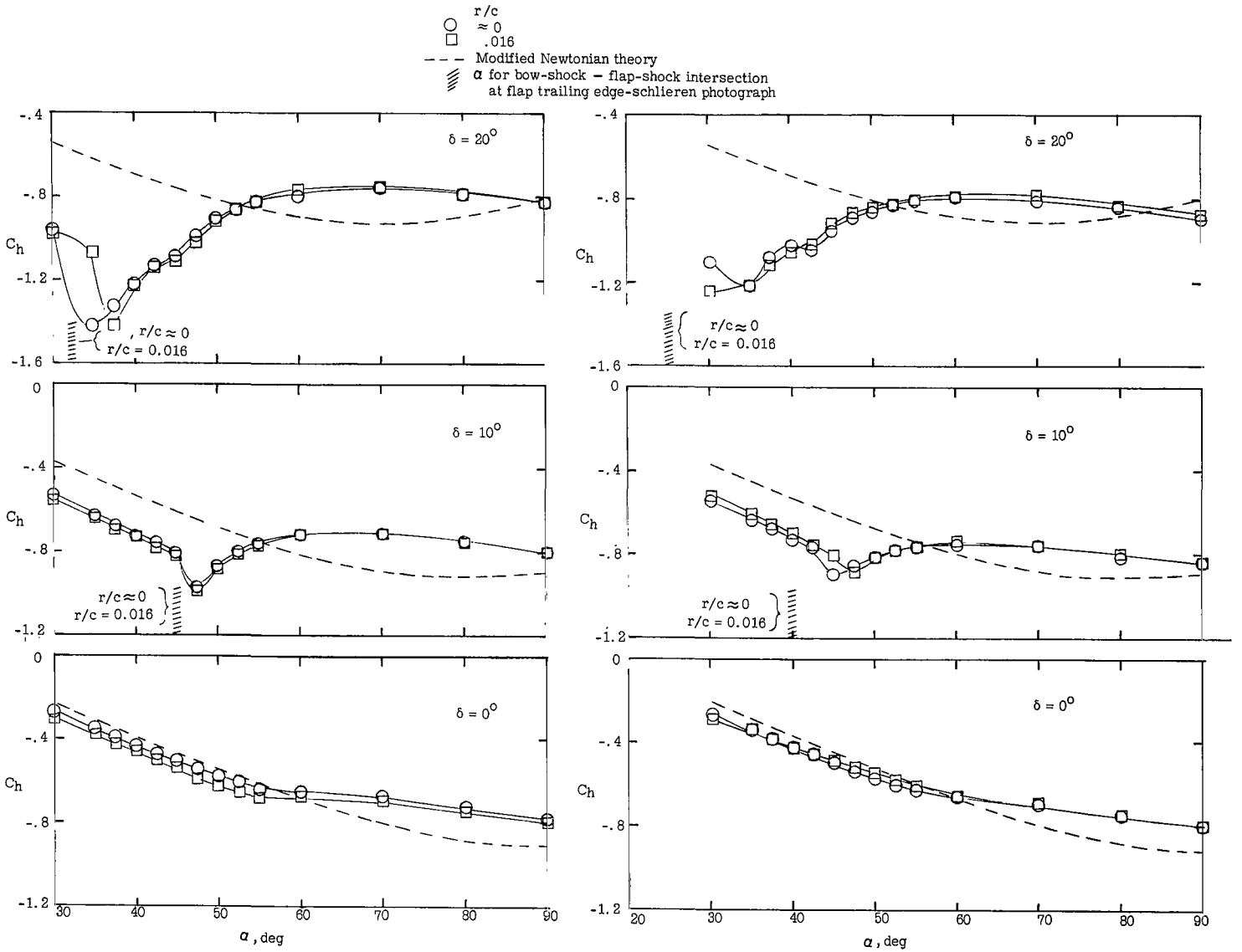

(a) A = 3.212.

(b) A = 2.143.

Figure 8.- Effect of delta-wing leading-edge bluntness on hinge-moment coefficient for both flap aspect ratios.

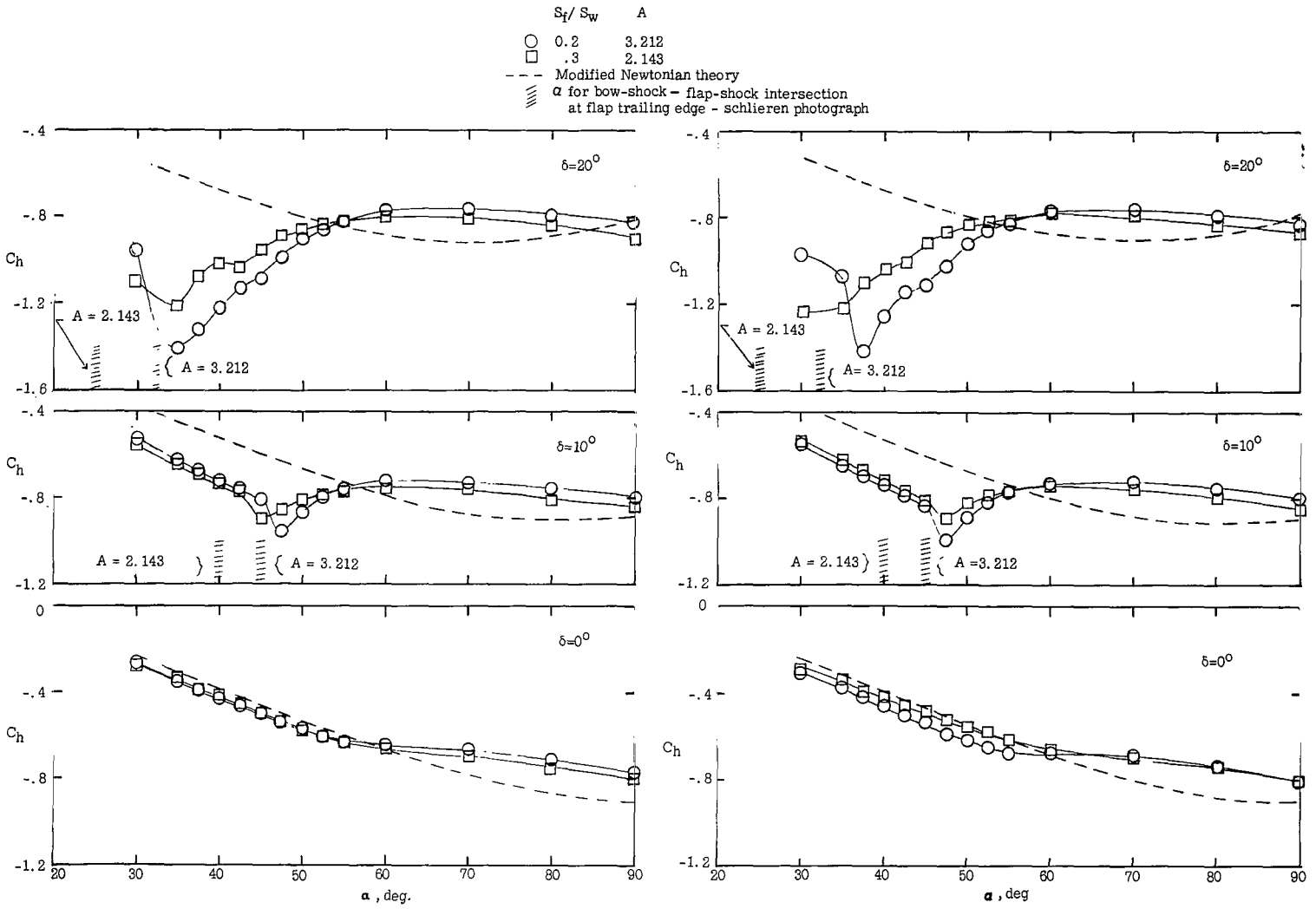

(a) r/c ≈ 0.

(b) r/c = 0.016.

Figure 9.- Effect of flap aspect ratio on hinge-moment coefficient for both leading-edge bluntnesses.

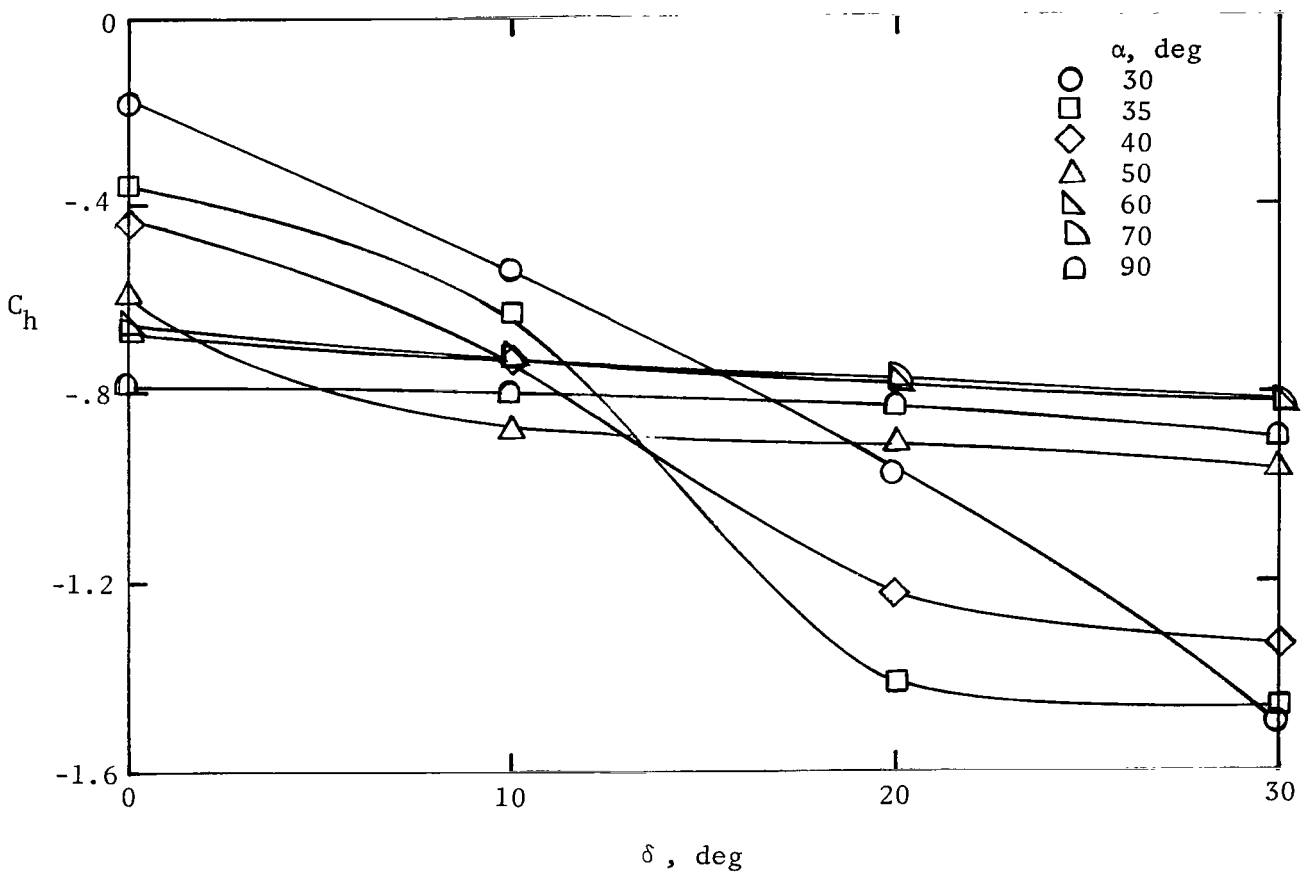

Figure 10.- Variation of hinge-moment coefficient as a function of flap-deflection angle. $r/c \approx 0$; A = 3.212.

NASA-Langley, 1967 —— 1 L-5020

"The aeronautical and space activities of the United States shall be conducted so as to contribute . . . to the expansion of human knowledge of phenomena in the atmosphere and space. The Administration shall provide for the widest practicable and appropriate dissemination of information concerning its activities and the results thereof."

—NATIONAL AERONAUTICS AND SPACE ACT OF 1958

NASA SCIENTIFIC AND TECHNICAL PUBLICATIONS

TECHNICAL REPORTS: Scientific and technical information considered important, complete, and a lasting contribution to existing knowledge.

TECHNICAL NOTES: Information less broad in scope but nevertheless of importance as a contribution to existing knowledge.

TECHNICAL MEMORANDUMS: Information receiving limited distribution because of preliminary data, security classification, or other reasons.

CONTRACTOR REPORTS: Scientific and technical information generated under a NASA contract or grant and considered an important contribution to existing knowledge.

TECHNICAL TRANSLATIONS: Information published in a foreign language considered to merit NASA distribution in English.

SPECIAL PUBLICATIONS: Information derived from or of value to NASA activities. Publications include conference proceedings, monographs, data compilations, handbooks, sourcebooks, and special bibliographies.

TECHNOLOGY UTILIZATION PUBLICATIONS: Information on technology used by NASA that may be of particular interest in commercial and other non-aerospace applications. Publications include Tech Briefs, Technology Utilization Reports and Notes, and Technology Surveys.

Details on the availability of these publications may be obtained from:

SCIENTIFIC AND TECHNICAL INFORMATION DIVISION

NATIONAL AERONAUTICS AND SPACE ADMINISTRATION

Washington, D.C. 20546